

Effects of disorder on polaritonic and dark states in a cavity using the disordered Tavis-Cummings model

Tarun Gera and K.L. Sebastian

Department of Inorganic and Physical Chemistry

Indian Institute of Science

Bangalore 560012

India

Abstract

We consider molecules confined to a microcavity whose dimensions are such that an excitation of the molecule is nearly resonant with a cavity mode. We investigate the situation where the excitation energies of the molecules are randomly distributed with a mean value of ϵ_a and variance σ . For this case, we find a solution that approaches the exact result for large values of the number density \mathcal{N} of the molecules. We find the conditions for the existence of the polaritonic states, as well as expressions for their energies. The polaritonic states are quite stable against disorder. Analytical results are verified by comparison with simulations. When ϵ_a is equal to that of the cavity state ϵ_c (on resonance) the gap between the two polaritonic states is found to increase with disorder, the increase being equal to $2\frac{\sigma^2}{\sqrt{\mathcal{N}|\tilde{V}|}}$ where \tilde{V} is the coupling of a molecular excitation to the cavity state. An analytic expression is found for the disorder induced width of the polaritonic peak. We results for various densities of states, and the absorption spectrum. The dark states that exist in the case $\sigma = 0$ turn “grey” in presence of disorder with their contribution to the absorption increasing with σ . We analyze the effect of including lifetimes of the cavity and molecular states and find that in the strong coupling regime, the width of the polaritonic peaks is dominated by the lifetime effect and that disorder plays almost no role, if the Rabi splitting is sufficiently large. We also consider the case where there is (a) orientational disorder as well as (b) spatial variation of the cavity field and find that they effectively amount to a renormalisation of the coupling.

I. INTRODUCTION

In the recent past, states of molecules confined in a micro-cavity have attracted much attention of chemists. The reason for this is that such confinement can lead to very interesting modifications of transport properties (energy and electron transfer reactions) and chemical reactivity. These happen when an excited state of the molecule is almost resonant with a cavity mode. In the strong coupling limit, modified chemical reactivity [1–5], site selectivity [2], altered enzyme activities [6] and enhanced rate of energy transfer [7–10] are some of the processes that have been reported. These applications of light-matter interactions in chemistry that have been reported confirms the presence of hybrid light-matter states, for organic dye molecules at room temperature in different states of matter confined in a cavity. The Ebbesen group has been working on such systems and has reported [1, 2, 6–8, 11–13] many studies with various applications. Other research groups also have recently published results [3–5, 9, 10, 14, 15] showing modified chemistry in such cavities. One of the phenomena which is of great interest is the modification in chemical reactivity, which can be achieved by making the cavity mode resonate with different vibrational modes of the molecules. Many theoretical models have been developed to understand this modified chemistry inside the cavity. Transition state theory has been used to explain this phenomenon but has not yet been able to provide a satisfactory explanation [16–18]. This shows the need of continuous exploration and development of theories which could explain the experimental results. The review articles [19–26] compile the past developments, current status and unanswered questions in this rapidly developing area of research.

When molecules are confined inside a cavity, there will be energy transfer between excited states of the molecules and the cavity mode of the confined electromagnetic field. If the rate of this energy exchange is fast enough polaritonic modes are formed. For N molecules confined to the cavity that couple to the cavity mode through their transition dipoles, the coupling leads to two polaritonic modes and $N - 1$ other states. In the case where all the molecules have identical excitation energies, these $(N - 1)$ modes are completely decoupled from the electromagnetic field and hence cannot be excited by radiation. Consequently, they are referred to as the “dark modes”. It is the formation of these mixed light+matter states that leads to the new phenomena. The polaritonic states have been predicted to lead to enhanced electron transfer rates for molecules confined in the cavity [27]. A very interesting

experimental demonstration is the energy transfer mediated by polaritons [7, 9].

For molecules put inside a cavity there would be disorder in the energy levels due to various reasons [28]. The causes may be inhomogeneities in the material, different levels of aggregation, dispersal by solvent or solvent fluctuations. It is well known that in general, transport properties are strongly affected by the presence of disorder. The reason for this is that disorder would in general cause the states to be localized (Anderson localization) rather than delocalized. For models in which one has nearest neighbour hopping, even a small disorder leads to localization in $1D$ (dimension) and $2D$. In $3D$ when the disorder exceeds a critical value the system would undergo metal-insulator transition. Many aspects of disordered systems confined to a cavity have been investigated, mostly by numerical methods by Schachenmayer et. al. [29]. They consider the effect of the cavity on the transport on disordered systems, with nearest neighbor hopping. When the disorder is large enough, the states are localized and they investigate the effect of the cavity on these localized states. They find that the dark states are converted into “grey states”. Further, increasing the coupling to the cavity increases delocalization. The states can be spread over multiple sites, which are not neighbors in space, but are in energy. They find that these “semi-localized” states obey a semi-Poisson statistics in the energy level spacings. Also, the coupling through cavity modes is non-local and hence the effects are not dependent on the dimensionality of the system. The semi-localized states are found to be responsible for diffusive-like dynamics. It has been suggested by Yuen-Zhou et al. [30] that the semi-localized states contribute significantly to vibrational cooling, which leads to significant enhancement of rate of electron transfer. In a new interesting work, Celardo et al. [31] explore the long range hopping where transport efficiency at first decreases, later increases and finally becomes invariant as disorder increases.

Most of the investigations do not consider the position or orientational dependence of the coupling of the molecule with the cavity mode, as they assume the coupling to be a constant. In addition, the inhomogeneities of the surrounding medium will affect the excitation energies, so that their values would be distributed randomly. Such disorder has been investigated previously in an interesting paper by Houdré et. al. [32]. Our analysis goes beyond theirs, in ways that are made clear in the Section IV of this paper. In the present work we study the effect of these disorders on the polaritonic and the dark states. Using the Tavis-Cummings Hamiltonian [33, 34] with added disorder, we analytically solve

for the Green's function for the system in the limit $N \gg 1$. The density of states and absorption cross-section also are analytically expressed in terms of the Green's function. In section III we consider the model where the coupling of each molecule to the cavity state is considered to be the same, but their excitation energies are randomly distributed. Having illustrated our approach with this simple model, in section V we discuss the more general case in which the coupling depends on the position as well as the orientation of the transition dipole moment of the molecule with respect to the cavity field. To see the effects of disorder clearly we have taken the lifetime of the excited molecular state to be very long. We also discuss the inclusion of lifetime effects. It is found that the polaritons have lifetimes which are weighted averages of the lifetimes of the cavity and the molecular states. Further, on resonance the disorder effects on the line-broadening are negligible if $\Omega \gg \frac{\gamma_a + \gamma_c}{2} \gg \sigma$, where Ω is the rabi splitting and γ_a and γ_c are the lifetimes of the molecular and cavity states.

II. THE HAMILTONIAN AND THE GREEN'S OPERATOR

In the Tavis-Cummings Hamiltonian [33, 34] with disorder in the excitation energies, we take the excitation energy ϵ_i of the i^{th} molecule to be

$$\epsilon_i = \epsilon_a + \xi_i, \quad (1)$$

where ξ_i is a random variable.

The total Hamiltonian may then be written as

$$\hat{H} = \epsilon_c |c\rangle\langle c| + \sum_i^N (\epsilon_a + \xi_i) |a_i\rangle\langle a_i| + \sum_i^N (V_i |c\rangle\langle a_i| + V_i^* |a_i\rangle\langle c|). \quad (2)$$

$|c\rangle$ denotes the state where the cavity mode is excited to its first excited state and it has an energy ϵ_c . $|a_i\rangle$ denotes the state in which the i^{th} molecule is excited with all the other molecules in their ground states. The coupling constant of the cavity mode to this excitation is denoted by V_i which is given by

$$V_i = -\mathbf{E}(z_i) \cdot \boldsymbol{\mu}_i = -\sqrt{\frac{\epsilon_c}{2\epsilon_o \mathcal{V}}} \mu_{eg} \sin(k_c z_i) \cos(\theta_i), \quad (3)$$

where \mathcal{V} is the volume of the cavity and $\boldsymbol{\mu}_i$ is transition dipole moment of the molecular excitation, having the magnitude μ_{eg} . The cavity field wave-vector and the permittivity

of free space are denoted as k_c and ϵ_o respectively. The term $\sin(k_c z_i)$ accounts for the spatial variation of the cavity field and θ_i is the angle between the transition dipole moment vector and the electric field vector. We use the Green's operator to analyze the problem following the techniques of the classic paper of Anderson on the impurity problem [35]. See also the book by Mattuck [36]. The Green's operator for the Hamiltonian \hat{H} is defined by $\hat{G}(\omega) = (\omega - \hat{H})^{-1}$, where ω is a complex variable. We shall calculate the matrix element $G_{ij}(\omega)$ of $\hat{G}(\omega)$ defined by

$$G_{ij}(\omega) = \langle i | \frac{1}{\omega - \hat{H}} | j \rangle, \quad (4)$$

where $|i\rangle$ and $|j\rangle$ are any two arbitrary states. $G_{ij}(\omega)$ has the spectral representation

$$G_{ij}(\omega) = \sum_m \frac{\langle i | \epsilon_m \rangle \langle \epsilon_m | j \rangle}{\omega - \epsilon_m}, \quad (5)$$

where $|\epsilon_m\rangle$ is an eigenfunction of the Hamiltonian operator having the eigenvalue ϵ_m , satisfying $\hat{H}|\epsilon_m\rangle = \epsilon_m|\epsilon_m\rangle$. Note that m runs from 1 to $(N + 1)$. From this it is clear that any discrete eigenvalue of \hat{H} appears as a simple pole of $G_{ij}(\omega)$ and that its residue at the pole at ϵ_m is $\langle i | \epsilon_m \rangle \langle \epsilon_m | j \rangle$, giving us an idea of the amount of contribution that the m^{th} eigenstate makes to $|i\rangle$ and $|j\rangle$. We now proceed to determine the matrix elements $G_{ij}(\omega)$.

The Hamiltonian may be written in the matrix form as

$$\underline{\underline{H}} = \left[\begin{array}{c|cccccc} \epsilon_c & V_1 & V_2 & \cdot & \cdot & \cdot & V_N \\ \hline V_1^* & \epsilon_1 & 0 & \cdot & \cdot & \cdot & 0 \\ V_2^* & 0 & \epsilon_2 & \cdot & \cdot & \cdot & 0 \\ \cdot & \cdot & \cdot & \cdot & \cdot & \cdot & \cdot \\ \hline V_N^* & 0 & 0 & \cdot & \cdot & \cdot & \epsilon_N \end{array} \right], \quad (6)$$

which has the partitioned form

$$\underline{\underline{H}} = \left[\begin{array}{c|c} \epsilon_c & \underline{V} \\ \hline \underline{V}^\dagger & \underline{\underline{\epsilon}}_M \end{array} \right]. \quad (7)$$

M stands for molecules and $\underline{V} = [V_1, V_2, \dots, V_N]$ is a row matrix having dimensions $1 \times N$. $\underline{\underline{\epsilon}}_M$ is an $N \times N$ diagonal matrix of the excitation energies:

$$\left(\underline{\underline{\epsilon}}_M \right)_{ij} = \epsilon_i \delta_{ij}. \quad (8)$$

The matrix corresponding to $\hat{G}(\omega)$ operator is

$$\underline{\underline{G}} = \left(\omega \underline{\underline{I}}_{N+1} - \underline{\underline{H}} \right)^{-1}. \quad (9)$$

\underline{I}_{N+1} is the $(N+1)$ dimensional identity matrix. \underline{G} too can be written in the same partitioned form as in Eq. (7):

$$\underline{G} = \left[\begin{array}{c|c} G_{cc} & \underline{G}_{cM} \\ \hline \underline{G}_{cM}^\dagger & \underline{G}_M \end{array} \right]. \quad (10)$$

Eq. (9) can be rearranged to get

$$(\omega \underline{I}_{N+1} - \underline{H}) \underline{G} = \underline{I}_{N+1}. \quad (11)$$

Using Eq. (7), Eq. (9) and Eq. (10) we get

$$\begin{pmatrix} \omega - \epsilon_c & -\underline{V} \\ -\underline{V}^\dagger & \omega \underline{I} - \underline{\epsilon}_M \end{pmatrix} \begin{pmatrix} G_{cc} & \underline{G}_{cM} \\ \underline{G}_{cM}^\dagger & \underline{G}_M \end{pmatrix} = \begin{pmatrix} 1 & 0 \\ 0 & \underline{I} \end{pmatrix}. \quad (12)$$

In the above \underline{I} is the $N \times N$ identity matrix. Eq. (12) is equivalent to the following four equations:

$$(\omega - \epsilon_c) G_{cc} - \underline{V} \underline{G}_{cM}^\dagger = 1 \quad (13)$$

$$(\omega - \epsilon_c) \underline{G}_{cM} - \underline{V} \underline{G}_M = 0 \quad (14)$$

$$-\underline{V}^\dagger G_{cc} + (\omega \underline{I} - \underline{\epsilon}_M) \underline{G}_{cM}^\dagger = 0 \quad (15)$$

$$-\underline{V}^\dagger \underline{G}_{cM} + (\omega \underline{I} - \underline{\epsilon}_M) \underline{G}_M = \underline{I}. \quad (16)$$

Solving Eq. (15) for $\underline{G}_{cM}^\dagger$ gives

$$\underline{G}_{cM}^\dagger = (\omega \underline{I} - \underline{\epsilon}_M)^{-1} \underline{V}^\dagger G_{cc}. \quad (17)$$

Using Eq. (17) in Eq. (13) and solving for G_{cc} leads to

$$G_{cc} = [\omega - \epsilon_c - \Sigma(\omega)]^{-1}, \quad (18)$$

with the self energy $\Sigma(\omega)$ defined by

$$\Sigma(\omega) = \sum_i \frac{V_i^* V_i}{\omega - \epsilon_i}. \quad (19)$$

We define the imaginary and real parts of the self energy by:

$$\Sigma_I(\omega) = -\pi \sum_i |V_i|^2 \delta(\omega - \epsilon_i)$$

and

$$\Sigma_R(\omega) = -\frac{1}{\pi} \mathcal{P} \int_{-\infty}^{\infty} d\epsilon \frac{\Sigma_I(\epsilon)}{\omega - \epsilon},$$

where \mathcal{P} stands for the principal value of the integral. It is useful to introduce the density of states for the disordered molecular states by

$$\rho_d(\xi) = \frac{1}{N} \sum_{i=1}^N \delta(\xi - \xi_i). \quad (20)$$

In the following we first consider the simplest possible model where $V_i = V$, a constant. For this model, all the calculations are reported in detail. After that we also discuss more general cases in section V.

III. MODEL I: $V_i = V$

We note that the coupling $V \propto \frac{1}{\sqrt{\mathcal{V}}}$, where \mathcal{V} is the volume of the cavity. We define \mathcal{N} the number density of molecules by $\mathcal{N} = N/\mathcal{V}$ is the number density of molecules and volume independent coupling $\tilde{V} = V\sqrt{\mathcal{V}}$.

We use the notation $\omega^+ = \omega + i\eta$ when ω is real and η is taken to be an infinitesimal positive number. We then have

$$\Sigma(\omega^+) = \mathcal{N}\tilde{V}^2 \int_{-\infty}^{\infty} d\xi \frac{\rho_d(\xi)}{\omega + i\eta - \epsilon_a - \xi}. \quad (21)$$

Separating out the real and imaginary parts of $\Sigma(\omega^+)$ gives

$$\Sigma(\omega^+) = \mathcal{N}\tilde{V}^2 \mathcal{P} \int_{-\infty}^{\infty} d\xi \frac{\rho_d(\xi)}{\omega - \epsilon_a - \xi} - i\pi \mathcal{N}\tilde{V}^2 \int_{-\infty}^{\infty} d\xi \rho_d(\xi) \delta(\omega - \epsilon_a - \xi), \quad (22)$$

where \mathcal{P} denotes the principal value of the integral.

In this simplest model with $V_i = V$, the coupling with the cavity field is the same for all molecules. Further we shall take ξ_i to be identically distributed Gaussian random variables with the probability distribution

$$P(\xi) = \frac{1}{\sqrt{2\pi}\sigma} e^{-\frac{\xi^2}{2\sigma^2}}. \quad (23)$$

In principle, one has to average over different realisations of the random quantities ξ_i . However when \mathcal{N} is large, we expect $\rho_d(\omega) \rightarrow P(\xi)$. Hence in this limit one expects *the ensemble averaged value* of self energies to be given by:

$$\Sigma_I(\omega) = \frac{\mathcal{N}\tilde{V}^2\pi}{\sqrt{2\pi}\sigma} e^{-\frac{(\omega-\epsilon_a)^2}{2\sigma^2}} \quad (24)$$

and

$$\Sigma_R(\omega) = \frac{\sqrt{2}\mathcal{N}\tilde{V}^2}{\sigma} DawsonF\left(\frac{\omega - \epsilon_a}{\sqrt{2}\sigma}\right). \quad (25)$$

$DawsonF(x)$ is the Dawson Integral (also referred to as Dawson function) [37], defined by

$$DawsonF(x) = e^{-x^2} \int_0^x dy e^{y^2}. \quad (26)$$

Using these results in Eq. (18) we get

$$G_{cc}(\omega) = \left[\omega - \epsilon_c - \frac{\sqrt{2}\mathcal{N}\tilde{V}^2}{\sigma} DawsonF\left(\frac{\omega - \epsilon_a}{\sqrt{2}\sigma}\right) + \frac{i\mathcal{N}\tilde{V}^2\pi}{\sqrt{2\pi}\sigma} e^{-\frac{(\omega - \epsilon_a)^2}{2\sigma^2}} \right]^{-1}. \quad (27)$$

A. The Density of States

We define the density of states for the cavity state by

$$\begin{aligned} \rho_c(\omega) &= \sum_{m=1}^{N+1} |\langle c|m\rangle|^2 \delta(\omega - \epsilon_m) \\ &= -\frac{1}{\pi} \text{Im}\{G_{cc}(\omega^+)\}. \end{aligned} \quad (28)$$

$\rho_c(\omega)$ gives us an idea of the amount of participation of the cavity state in the m^{th} eigenstate of the system.

Now we calculate the matrix elements of Green's operator for the molecular states. Eq. (15) can be solved for \underline{G}_{cM} to get

$$\underline{G}_{cM} = (\omega - \epsilon_c)^{-1} \underline{V} \underline{G}_M. \quad (29)$$

Using this result in Eq. (16) gives

$$\underline{G}_M(\omega^+) = \left[\underline{I}\omega^+ - \underline{\epsilon}_M - \frac{\underline{V}^\dagger \underline{V}}{\omega^+ - \epsilon_c} \right]^{-1}. \quad (30)$$

The operator corresponding to the matrix $\underline{V}^\dagger \underline{V}$ can be written in the form $\mathcal{N}\tilde{V}^2 |mol\rangle \langle mol|$ with

$$|mol\rangle = \frac{1}{\sqrt{N}} \sum_{i=1}^N |i\rangle. \quad (31)$$

Hence we can write the operator corresponding to the matrix $\underline{G}_M(\omega^+)$ as

$$\hat{G}_M(\omega^+) = \left[\omega^+ - \hat{\epsilon}_M - \frac{\mathcal{N}\tilde{V}^2 |mol\rangle \langle mol|}{\omega^+ - \epsilon_c} \right]^{-1}. \quad (32)$$

The operator $\hat{\epsilon}_M$ is defined by its matrix elements $\langle i|\hat{\epsilon}_M|i'\rangle = \epsilon_i \delta_{ii'}$. Using the operator identity $(\hat{A} - \hat{B})^{-1} = \hat{A}^{-1} + \hat{A}^{-1}\hat{B}(\hat{A} - \hat{B})^{-1}$ valid for any two operators \hat{A} and \hat{B} , we can write

$$\hat{G}_M(\omega^+) = [\omega^+ - \hat{\epsilon}_M]^{-1} + [\omega^+ - \hat{\epsilon}_M]^{-1} \frac{\mathcal{N}\tilde{V}^2 |mol\rangle \langle mol|}{\omega^+ - \epsilon_c} \hat{G}_M(\omega^+). \quad (33)$$

From this we find $\langle mol|\hat{G}_M(\omega^+)$ to obey the equation

$$\langle mol|\hat{G}_M(\omega^+) = \langle mol| [\omega^+ - \hat{\epsilon}_M]^{-1} + \frac{\Sigma(\omega^+)}{(\omega^+ - \epsilon_c)} \langle mol|\hat{G}_M(\omega^+). \quad (34)$$

Solving for $\langle mol|\hat{G}_M(\omega^+)$ gives

$$\langle mol|\hat{G}_M(\omega^+) = (\omega^+ - \epsilon_c) G_{cc}(\omega^+) \langle mol| [\omega^+ - \hat{\epsilon}_M]^{-1}.$$

Using this back in Eq. (33) we get

$$\hat{G}_M(\omega^+) = [\omega^+ - \hat{\epsilon}_M]^{-1} + [\omega^+ - \hat{\epsilon}_M]^{-1} \mathcal{N}\tilde{V}^2 |mol\rangle G_{cc}(\omega^+) \langle mol| [\omega^+ - \hat{\epsilon}_M]^{-1}. \quad (35)$$

Using the above, the matrix element $G_{mol,mol}(\omega^+) = \langle mol|\hat{G}_M(\omega^+) |mol\rangle$ can be calculated to be:

$$G_{mol,mol}(\omega^+) = \left\{ 1 - \frac{\mathcal{N}\tilde{V}^2}{\omega^+ - \epsilon_c} \langle mol| (\omega^+ - \hat{\epsilon}_M)^{-1} |mol\rangle \right\}^{-1} \langle mol| (\omega^+ - \hat{\epsilon}_M)^{-1} |mol\rangle \quad (36)$$

$$= (\omega^+ - \epsilon_c) G_{cc}(\omega^+) \frac{1}{\mathcal{N}\tilde{V}^2} \Sigma(\omega^+). \quad (37)$$

From $G_{mol,mol}(\omega^+)$ we can calculate the density of states of $|mol\rangle$:

$$\rho_{mol}(\omega) = -\frac{1}{\pi} \text{Im}\{G_{mol,mol}(\omega^+)\}. \quad (38)$$

The total density of states may be defined by $\rho_T(\omega) = \sum_{m=1}^{N+1} \delta(\omega - \epsilon_m)$ which may be written as $\rho_T(\omega) = -\frac{1}{\pi} \text{Im}\left(\text{Tr}\hat{G}(\omega^+)\right)$. Using the complete set $|c\rangle, |1\rangle, |2\rangle, \dots, |N\rangle$ to calculate the trace leads to

$$\rho_T(\omega) = \rho_c(\omega) - \sum_{i=1}^N \frac{1}{\pi} \text{Im}\{G_{ii}(\omega^+)\}, \quad (39)$$

with $G_{ii}(\omega^+) = \langle i|\hat{G}(\omega^+)|i\rangle$. $G_{ii}(\omega^+)$ for $i \neq c$ may be easily evaluated using Eq. (35), to get

$$G_{ii}(\omega^+) = (\omega^+ - \epsilon_i)^{-1} + V^2(\omega^+ - \epsilon_i)^{-2} G_{cc}(\omega^+),$$

so that

$$\sum_{i=1}^N G_{ii}(\omega^+) = \sum_{i=1}^N (\omega^+ - \epsilon_i)^{-1} + V^2 G_{cc}(\omega^+) \sum_{i=1}^N (\omega^+ - \epsilon_i)^{-2}. \quad (40)$$

A change in the total density of states for the molecules alone may be defined by

$$\Delta\rho_M(\omega) = -\frac{1}{\pi} \text{Im} \left(\sum_{i=1}^N G_{ii}(\omega^+) \right) - \rho_M^0(\omega),$$

where $\rho_M^0(\omega)$ is the density of molecular states in the case where $\tilde{V} = 0$. The above may be calculated using Eq. (40) to be

$$\Delta\rho_M(\omega) = \frac{1}{\pi} \text{Im} \left(\frac{\partial \Sigma(\omega^+)}{\partial \omega} G_{cc}(\omega^+) \right) \quad (41)$$

so that the change in the total density of states, due to the interaction of the cavity mode with the molecules is

$$\Delta\rho_T(\omega) = -\frac{1}{\pi} \text{Im}\{G_{cc}(\omega^+)\} - \frac{1}{\pi} \text{Im}\left\{\frac{\partial \Sigma(\omega^+)}{\partial \omega} G_{cc}(\omega^+)\right\}. \quad (42)$$

B. The Absorption Spectrum

The Hamiltonian for the interaction of the system with radiation is

$$\hat{H}_{int}(t) = - \sum_i \mathbf{E}_i(t) \cdot \hat{\boldsymbol{\mu}}_i.$$

The $\hat{\boldsymbol{\mu}}_i$ operator can be written in terms in terms of transition dipole moment as:

$$\hat{\boldsymbol{\mu}}_i = \boldsymbol{\mu}_i |g\rangle \langle i| + \boldsymbol{\mu}_i^* |i\rangle \langle g|$$

where $\boldsymbol{\mu}_i = \langle i | \hat{\boldsymbol{\mu}}_i | g \rangle$. We can rewrite the Hamiltonian for interaction as:

$$\hat{H}_{int}(t) = - \sum_i \mathbf{E}_i(t) \cdot (\boldsymbol{\mu}_i |g\rangle \langle i| + \boldsymbol{\mu}_i^* |i\rangle \langle g|). \quad (43)$$

$|g\rangle$ indicates the ground state in which all the molecules are in their ground states. $|i\rangle$ is the site in which the i^{th} molecule is excited. $\mathbf{E}_i(t)$ is the harmonic electric field of the frequency ω that the i^{th} molecule experiences. In the spirit of the model that assumes $V_i = V$ a constant, we first take the electric field to be the same for all the molecules - i.e., neglect its space dependence so that all the molecules experience the same electric field. Further,

for simplicity, we take all of them to be oriented in the direction of the electric field. Under these assumptions,

$$\hat{H}_{int}(t) = - \sum_i E(t) (\mu_{eg}|g\rangle\langle i| + \mu_{ge}^*|i\rangle\langle g|)$$

where $\mu_{eg} = |\boldsymbol{\mu}_i|$ and $E(t)$ is the electric field in the direction of the transition dipole of i^{th} molecule. The absorption cross section $\alpha(\omega)$ for radiation of frequency ω is then

$$\alpha(\omega) = \frac{\pi\omega}{\epsilon_o c \hbar} \sum_f \left| \langle f | \hat{H}_{int}(0) | g \rangle \right|^2 \delta(E_f - E_g - \hbar\omega).$$

In the above, E_g is the energy of the ground state. $|f\rangle$ denotes a possible final state, having energy E_f . Following reference [38] we write this as the Fourier transform of a correlation function:

$$\alpha(\omega) = \frac{\omega}{2\epsilon_o c \hbar} \int_{-\infty}^{\infty} dt e^{i\omega t} \langle g | \hat{H}_{int}(t) \hat{H}_{int} | g \rangle,$$

where $\hat{H}_{int}(t) = e^{i\hat{H}t/\hbar} \hat{H}_{int}(0) e^{-i\hat{H}t/\hbar}$. On using the expression for H_{int} and simplifying we get

$$\begin{aligned} \alpha(\omega) &= \frac{\omega}{2\epsilon_o c \hbar} |\boldsymbol{\mu}|^2 \int_{-\infty}^{\infty} dt e^{i\omega t} \sum_{i,j} \langle i | e^{i\hat{H}t/\hbar} | j \rangle \\ &= -\frac{\omega}{\epsilon_o c \hbar} N |\boldsymbol{\mu}|^2 \text{Im} [G_{mol,mol}(\omega)]. \end{aligned} \quad (44)$$

IV. RESULTS

A. Existence of polaritonic states

We now analyze $G_{cc}(\omega)$ to see the effect of disorder on the polaritonic states. At small disorder one expects the polaritonic states to exist. However, as the disorder increases, one suspects that the polaritonic states may disappear. For the sake of simplicity we consider only the case where $\epsilon_c = \epsilon_a$, and it is easy to extend the analysis to more general cases. In the following we make a quantitative analysis using the figures 1 and 2, which differ in their values of \mathcal{N} . Both show the plots of $\omega - \epsilon_c$, $\Sigma_R(\omega - \epsilon_c)$ and $\Sigma_I(\omega - \epsilon_c)$ against $\omega - \epsilon_c$. A pole of $G_{cc}(\omega)$ occurs at a point where the plot of $\omega - \epsilon_c$ intersects with that of $\Sigma_R(\omega - \epsilon_c)$. Fig. 1 is for large values of \mathcal{N} and in this case there are three points where this happens. The intersection at the origin has a large value for the imaginary part $\Sigma_I(\omega - \epsilon_c)$ implying that this is a virtual state. The other two intersections have only a small value of $\Sigma_I(\omega - \epsilon_c)$

indicating these are the long lived polaritonic states. This figure is to be compared with Fig. 2 which is for smaller values of \mathcal{N} or larger value of σ . In this case the polaritonic states do not exist. Only the virtual state is there. The plot of $\Sigma_R(\omega - \epsilon_c)$ has a slope of $\frac{\mathcal{N}\tilde{V}^2}{\sigma^2}$ at $\omega = \epsilon_c$. Hence the two polaritonic poles can exist only if $\frac{\mathcal{N}\tilde{V}^2}{\sigma^2} > 1$. For suitable values of the parameters, it is also possible that only one polaritonic state exists.

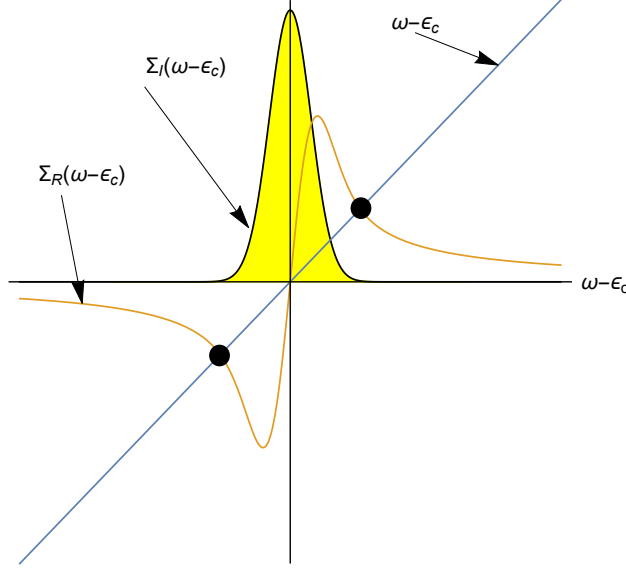


Figure 1: This figure takes ϵ_a to be equal to ϵ_c . The plots of $\omega - \epsilon_c$, $\Sigma_R(\omega - \epsilon_c)$ and $\Sigma_I(\omega - \epsilon_c)$ against $(\omega - \epsilon_c)$. The darkened small circles indicate points where $\omega - \epsilon_c$ intersects with $\Sigma_R(\omega - \epsilon_c)$ leading to the formation of two discrete poles. These correspond to the polaritonic states. The intersection at the origin indicates a virtual state as the imaginary part of the self energy $\Sigma_I(0)$ is large at this point.

We now make an analysis that is valid for arbitrary values of ϵ_a and ϵ_c . We consider the case where disorder is not large so that the situation in Fig. 1 occurs and there are two poles for $G_{cc}(\omega)$. These poles occur for large values of $|\omega - \epsilon_c|$ and $|\omega - \epsilon_a|$. The Dawson Function has the asymptotic form

$$DawsonF(x) = \frac{1}{2x} + \frac{1}{4x^3} + \frac{3}{8x^5} + O\left(\frac{1}{x^7}\right) \quad \text{for } |x| \text{ large.}$$

Using this to the lowest order (i.e. only the $1/x$ term is retained), we find that for $\left|\frac{\omega - \epsilon_a}{\sqrt{2}\sigma}\right| \gg 1$, $\frac{\sqrt{2}\mathcal{N}\tilde{V}^2}{\sigma} DawsonF\left(\frac{\omega - \epsilon_a}{\sqrt{2}\sigma}\right) \simeq \frac{\mathcal{N}\tilde{V}^2}{(\omega - \epsilon_a)}$ and hence

$$G_{cc}(\omega) = \left(\omega - \epsilon_c - \frac{\mathcal{N}\tilde{V}^2}{(\omega - \epsilon_a)} + i \frac{\mathcal{N}\tilde{V}^2\pi}{\sqrt{2\pi}\sigma} e^{-\frac{(\omega - \epsilon_a)^2}{2\sigma^2}} \right)^{-1}.$$

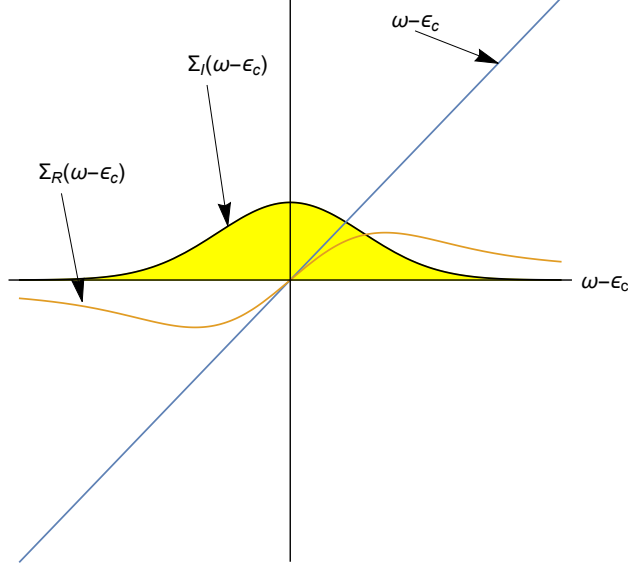


Figure 2: This figure takes ϵ_a to be equal to ϵ_c . The plots of $\omega - \epsilon_c$, $\Sigma_R(\omega - \epsilon_c)$ and $\Sigma_I(\omega - \epsilon_c)$ against $(\omega - \epsilon_c)$ for increased disorder. There is only one point where $\omega - \epsilon_c$ intersects with $\Sigma_R(\omega - \epsilon_c)$ and that is just the virtual state.

As $(\omega - \epsilon_a)/(\sqrt{2}\sigma) \gg 1$, the imaginary part in the above is very small and may be neglected for a first analysis. Then $G_{cc}(\omega)$ has poles at ϵ_{\pm} given by

$$\epsilon_{\pm} = \frac{(\epsilon_a + \epsilon_c)}{2} \pm \sqrt{\mathcal{N}\tilde{V}^2 + \left(\frac{\epsilon_a - \epsilon_c}{2}\right)^2}. \quad (45)$$

These are the two polaritonic states $|+\rangle$ and $|-\rangle$. The similarity of the above to simple molecular orbital theory [39] is to be noted. The residues of these at the poles are easily found to be

$$|\langle c|\pm\rangle|^2 = \left[1 + \frac{\mathcal{N}\tilde{V}^2}{(\epsilon_{\pm} - \epsilon_a)^2}\right]^{-1}.$$

For $\sqrt{\mathcal{N}}|\tilde{V}| \gg |\epsilon_c - \epsilon_a|$ these reduce to

$$\epsilon_{\pm} \simeq \frac{(\epsilon_a + \epsilon_c)}{2} \pm |\tilde{V}|\sqrt{\mathcal{N}}$$

and

$$|\langle c|\pm\rangle|^2 \simeq \frac{1}{2}.$$

At these poles, the imaginary part $[G_{cc}(\omega)]^{-1}$ can be easily estimated to be $\approx i\frac{\mathcal{N}\tilde{V}^2\pi}{\sqrt{2\pi}\sigma}e^{-\frac{\mathcal{N}\tilde{V}^2}{2\sigma^2}}$. This gives the width of the polaritonic peaks. Note that the width of the peak is decreasing

exponentially with \mathcal{N} and hence its height would increase exponentially.

From Eq. (45) we see the independence of ϵ_{\pm} upto first order in σ . To see the effect of disorder, it is necessary to do an analysis up to second order in σ . Under the assumption that the imaginary part is small and keeping the next two terms too in the asymptotic expansion of $DawsonF(x)$ we can find solutions for ϵ_{\pm} up to order σ^2 using MATHEMATICA to be

$$\epsilon_s = \frac{(\epsilon_a + \epsilon_c)}{2} + s \sqrt{\mathcal{N}\tilde{V}^2 + \left(\frac{\epsilon_a - \epsilon_c}{2}\right)^2} + s \frac{\sigma^2 \left(\left(\frac{\epsilon_a - \epsilon_c}{2}\right) \left(\frac{\epsilon_a - \epsilon_c}{2} + s \sqrt{\mathcal{N}\tilde{V}^2 + \left(\frac{\epsilon_a - \epsilon_c}{2}\right)^2}\right) + \mathcal{N}\tilde{V}^2 \right)}{\mathcal{N}\tilde{V}^2 \sqrt{\mathcal{N}\tilde{V}^2 + \left(\frac{\epsilon_a - \epsilon_c}{2}\right)^2}}, \quad (46)$$

where $s = \pm$. For $\epsilon_c = \epsilon_a$ this reduces to

$$\epsilon_{\pm} = \epsilon_c \pm \left(\sqrt{\mathcal{N}}|V| + \frac{\sigma^2}{\sqrt{\mathcal{N}}|V|} \right). \quad (47)$$

Thus when $\epsilon_a = \epsilon_c$, the gap between the two polaritonic states is increased by the disorder, a conclusion which is valid to order σ^2 . Further, as the number of molecules increase, the effects of disorder on the polaritonic states decrease. These results indicate that the polaritons are quite stable even in the presence of disorder, provided the number density of molecules is large enough, i.e., when $\sqrt{\mathcal{N}}|\tilde{V}| \gg \sigma$, a condition that is satisfied easily. It may be noted that an analysis valid up to first order in ξ was performed in the paper by Houdré [32], who concluded that disorder has no effect on the separation between the polaritonic states. In our notation, their analysis corresponds to doing calculations correct up to first order in σ . From the above it is clear that at this order in σ , disorder has no effect on the separation between the polaritonic peaks, in agreement with them.

1. Testing analytical results using simulations

We perform numerical calculations to determine the density of states using the equations given in previous sections. For this we generated \mathcal{N} values of ξ_i using a Gaussian distribution with zero mean and standard deviation σ . In principle, we should solve for the roots of $(\omega - \epsilon_c - \Sigma_R(\omega))$ and then construct the plot. We can easily bypass this by assuming that ω has a small imaginary part and then calculating $-\frac{1}{\pi} \text{Im}[G_{cc}(\omega)]$. In our calculations, we have taken the imaginary part to be equal to $0.001eV$. The resulting plot is not very sensitive

to the value of this imaginary part. All the other quantities of interest are evaluated in a similar fashion. For each quantity we average over 3000 realizations. In Fig. 3, 4 and 5 one can observe the good agreement between the simulations and the theoretical results even for \mathcal{N} as small as $\mathcal{N} = 1500 m^{-3}$. Fig. 3 shows the close agreement between theoretically calculated $\rho_c(\omega)$ with the one obtained from simulations. In Fig. 4 we show plots of $\rho_T(\omega)$ against ω for two values of σ . Because of the division by \mathcal{N} the polaritonic peaks have a small height and are not clearly visible. Fig. 5 shows the comparison of the analytical and

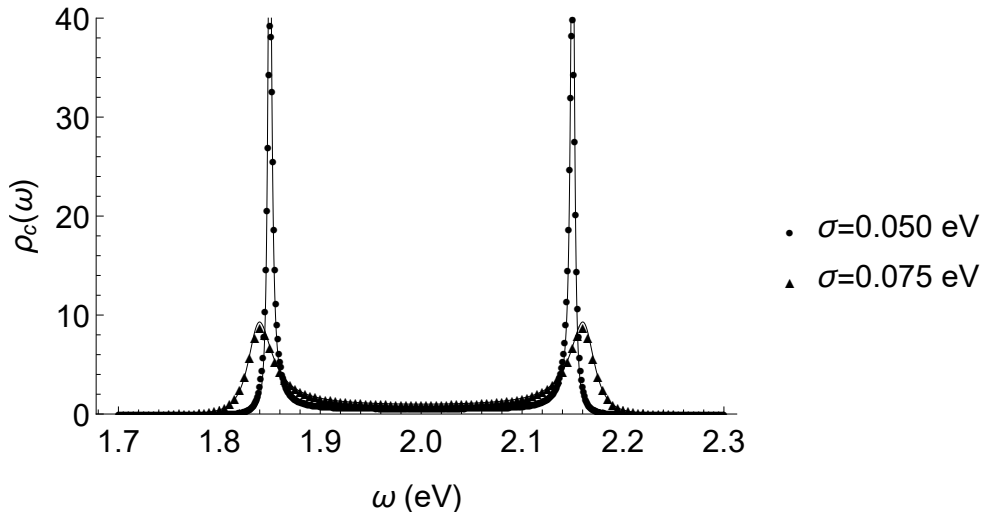


Figure 3: Plot of $\rho_c(\omega)$ against ω for $\mathcal{N} = 1500 m^{-3}$. Following values were used: $\epsilon_c = 2.0 eV$, $\epsilon_a = 2.0 eV$, $\tilde{V} = 3.56 \times 10^{-3} eV m^{3/2}$ and $\eta = 0.001 eV$. The points represents the simulations and the line plot is for the analytical result.

simulated results for $-\frac{1}{\pi}Im[G_{mol,mol}(\omega)]$. The agreement between the two is good.

Having illustrated the results using smaller values of \mathcal{N} , we now extend our results to experimentally viable values, which are too large to be simulated. As our analysis becomes better and better with increase in \mathcal{N} one expects the analytical results to be accurate for such large values of \mathcal{N} . In Fig. 6 we plot $\rho_c(\omega)$ against ω for $\sigma = 0.01\epsilon_a, 0.03\epsilon_a$ and $0.05\epsilon_a$. The peak heights for the plot corresponding to $\sigma = 0.01\epsilon_a$ value is of the order of 10^9 and hence the top portion has been cutoff. The plots show that the polaritonic states are very much affected by the disorder, as seen from the analytical estimate of their widths which is of the order of $\approx \frac{\mathcal{N}\tilde{V}^2\pi}{\sqrt{2\pi\sigma}}e^{-\frac{\mathcal{N}\tilde{V}^2}{2\sigma^2}}$.

In Fig. 7 we plot $\rho_T(\omega)/\mathcal{N}$ vs ω for experimentally viable values for different values of σ . One does not see the polaritonic peaks in this plot because the height and width of those

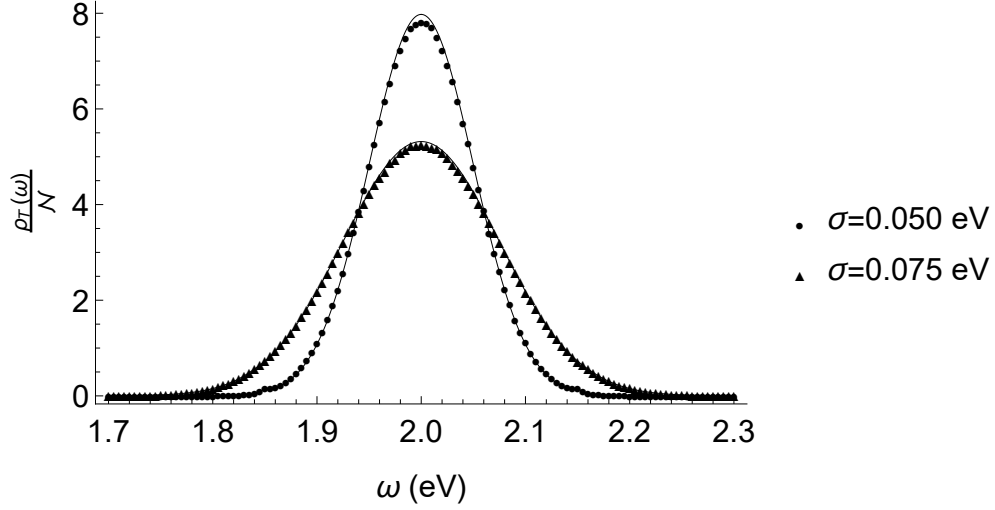


Figure 4: Plot of $\rho_T(\omega)/\mathcal{N}$ against ω for $\mathcal{N} = 1500 \text{ m}^{-3}$. Following values were used $\epsilon_c = 2.0 \text{ eV}$, $\epsilon_a = 2.0 \text{ eV}$, $\tilde{V} = 3.56 \times 10^{-3} \text{ eV m}^{3/2}$ and $\eta = 0.001 \text{ eV}$. The points represent the simulations and the line plot is for the theoretical result. The polaritonic peaks barely visible in the plot, due to the division by \mathcal{N} .

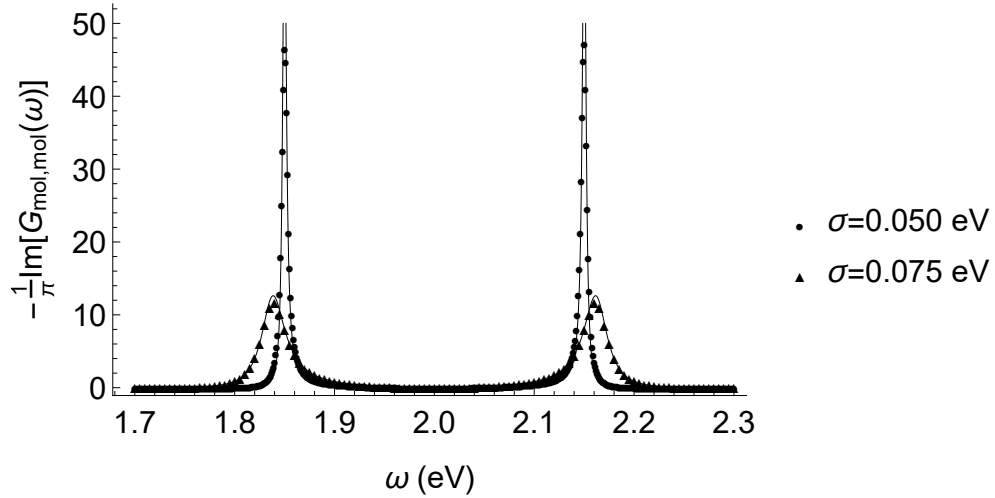


Figure 5: Plot of $-\frac{1}{\pi} \text{Im}[G_{mol,mol}(\omega)]$ against ω for $\mathcal{N} = 1500 \text{ m}^{-3}$. Following values were used: $\epsilon_c = 2.0 \text{ eV}$, $\epsilon_a = 2.0 \text{ eV}$, $\tilde{V} = 3.56 \times 10^{-3} \text{ eV m}^{3/2}$ and $\eta = 0.001 \text{ eV}$. The solid points represent the simulations and the line plot is for the analytical result.

two peaks are very small for all values of σ .

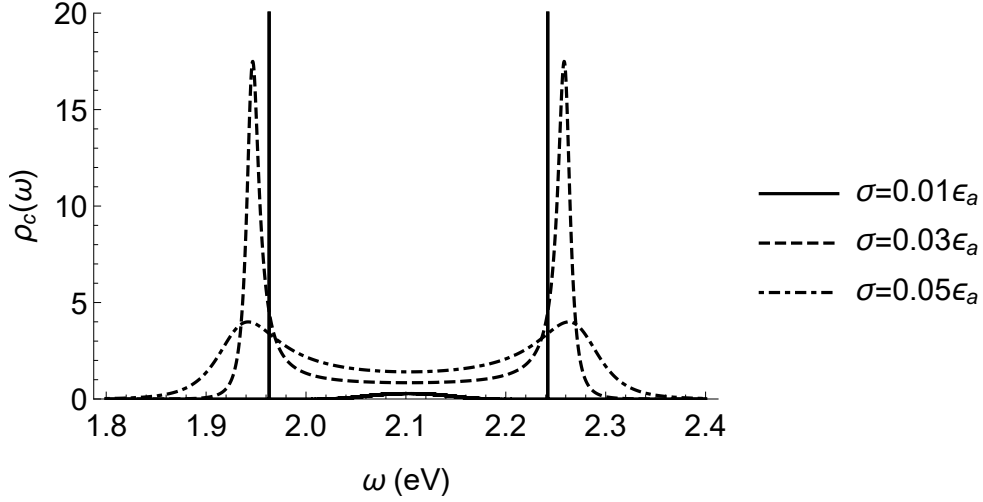


Figure 6: Plot for $\rho_c(\omega)$ v/s ω for $\mathcal{N} = 1.15 \times 10^{25} m^{-3}$ and for different values of σ .

Following values were used: $\epsilon_c = 2.1 eV$, $\epsilon_a = \epsilon_c$, $\tilde{V} = 4.06 \times 10^{-14} eVm^{3/2}$.

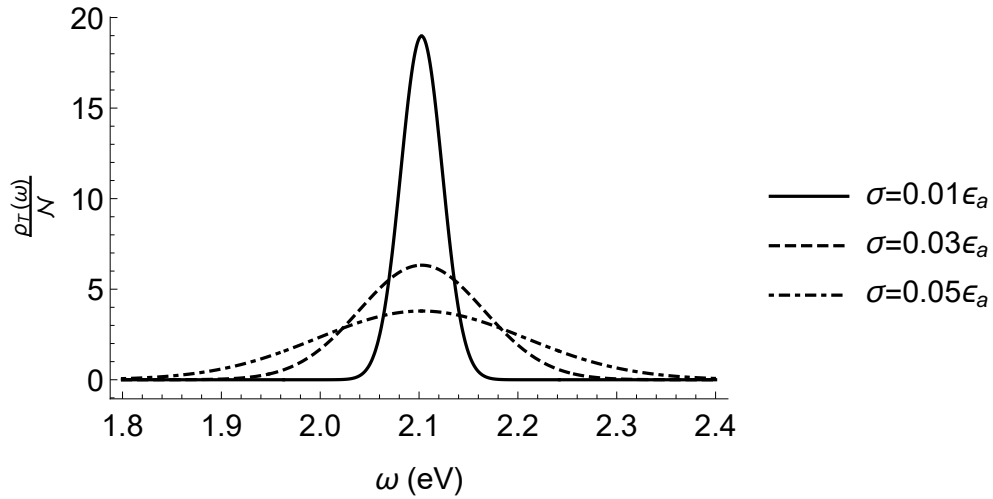


Figure 7: Plot for $\rho_T(\omega)/\mathcal{N}$ v/s ω for $\mathcal{N} = 1.15 \times 10^{25} m^{-3}$ and for different values of σ .

Following values were used: $\epsilon_c = 2.1 eV$, $\epsilon_a = \epsilon_c$, $\tilde{V} = 4.06 \times 10^{-14} eVm^{3/2}$.

2. Change in the density of states

Using the expression for the change in density of states given in Eq. (41) we plot $\Delta\rho_M(\omega)$ in Fig. 8. Integrating the area under the curve from $\omega = 2.0 eV$ to $\omega = 2.2 eV$ results in the value of -1 . This is what one would expect, because effectively out of the N molecular states 1 is used up for the formation of the two polaritonic states. The plot has a minimum at the middle. This is because it is the molecular states that are near resonance with the

cavity state that contribute the most to the polaritonic states and hence the depletion of density of $\rho_M(\omega)$ is maximum in the middle. In this figure, for $\sigma = 0.01\epsilon_a$ the polaritonic peaks are very high (height $\approx 10^9$) peak with a very narrow (width $\approx 10^{-10}$).

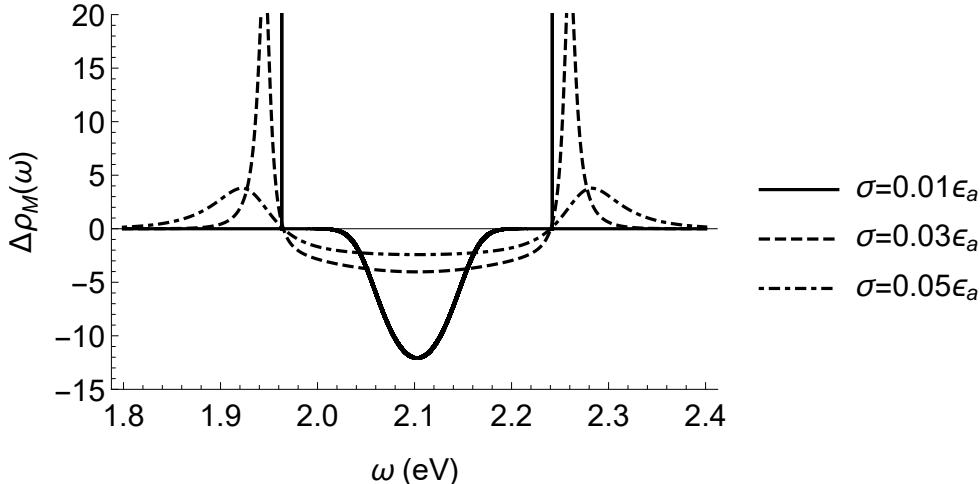


Figure 8: Plot of change in molecular density of states $\Delta\rho_M(\omega)$ vs ω for $\mathcal{N} = 1.16 \times 10^{25} m^{-3}$ and varied values of σ . Following values were used: $\epsilon_c = 2.1 eV$, $\epsilon_a = \epsilon_c$, $\tilde{V} = 4.06 \times 10^{-14} eVm^{3/2}$.

3. Absorption Cross Section

In Fig. 9 we plot the absorption cross-section given by Eq. (59) for increasing values of σ . The shift of peak position with increasing values of σ is clearly seen. In addition the peaks get broader as σ increases. This indicates that with increase in disorder, the dark states are turning “turning grey”. The dependence of width on σ is highly non-linear. The approximate relation between σ and the width, determined from the imaginary part of $[G_{cc}(\omega)]^{-1}$ at the poles, is $\approx \frac{\mathcal{N}\tilde{V}^2\pi}{\sqrt{2\pi\sigma}}e^{-\frac{\mathcal{N}\tilde{V}^2}{2\sigma^2}}$. When $\sigma \ll 2\sqrt{\mathcal{N}\tilde{V}}$ with $\sigma = 0.01\epsilon_a = 0.02 eV$ and $2\sqrt{\mathcal{N}\tilde{V}} = 0.275 eV$, contribution of the dark states to the absorption spectra is miniscule. The absorption is mostly from the two polaritonic states and amounts to 99.86% of the total and the absorption due to the grey states amounts to 0.14% when $\sigma = 0.01\epsilon_a$. For $\sigma = 0.01\epsilon_a$, the FWHM for the peaks corresponding to the two polaritonic states is of the order of $10^{-10} eV$ and peak height is of the order of 10^9 . As we increase the value of σ from $\sigma = 0.01 eV$ to $\sigma = 0.05\epsilon_a = 0.10eV$ the contribution of the dark states to the

absorption spectra steadily increases.

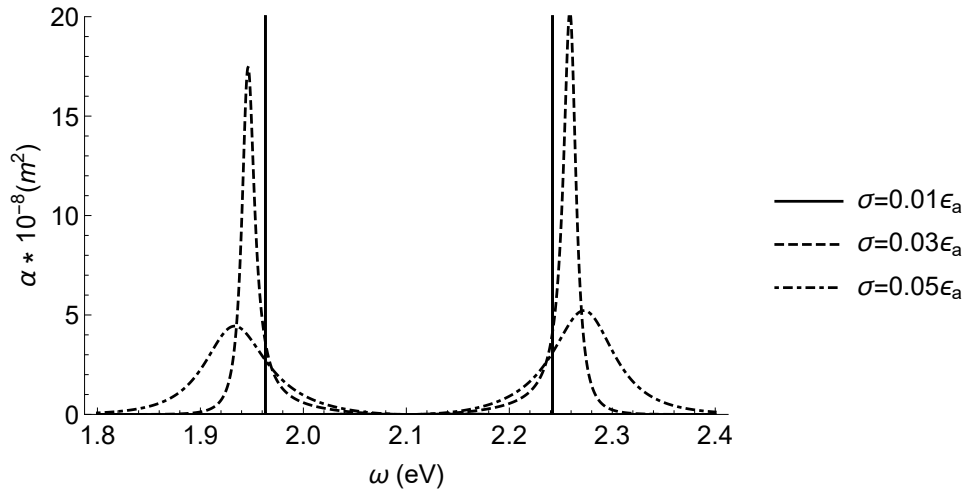


Figure 9: Plot of α against ω for $\mathcal{N} = 1.15 \times 10^{25} m^{-3}$ with varied values of σ . Following values were used: $\epsilon_c = 2.1 eV$, $\epsilon_a = \epsilon_c$, $\tilde{V} = 4.06 \times 10^{-14} eV m^{3/2}$ and $|\mu| = 10 D$. For the sake of clarity of the figure, the y-axis is cutoff at the value of 20. The peak height for $\sigma = 0.01\epsilon_a$ is of the order of 10^{10} .

4. Lifetime effects

Untill now we considered only the disorder as the source of line broadening. In this section we add the effect of homogeneous broadening for the molecular states (γ_a) and the cavity mode linewidth (γ_c). For this, we replace ϵ_c by $\epsilon_c - i\gamma_c$ and ϵ_a by $\epsilon_a - i\gamma_a$. Then the poles of the $G_{cc}(\omega)$ are at

$$\epsilon_{\pm} = \frac{1}{2} \left(\epsilon_a + \epsilon_c - i(\gamma_a + \gamma_c) \pm \sqrt{(-\epsilon_a + \epsilon_c + i(\gamma_a - \gamma_c))^2 + 4\mathcal{N}\tilde{V}^2} \right). \quad (48)$$

The above expression shows that the polaritons have lifetimes which are appropriately weighted averages of the lifetimes of the cavity and the molecular states, and that for large \mathcal{N} , disorder effects on the line-broadening are negligible.

For typical value of $\gamma_a = 10 ps$ ($0.3 meV$) and $\gamma_c = 40 fs$ ($0.1 eV$), we study the effect on the lineshape with increasing Rabi-splitting ($\Omega = 2\sqrt{\mathcal{N}\tilde{V}}$), shown in Fig. 10. In the previous section we stated that as \mathcal{N} increases the width of the polaritonic peaks exponentially decreases $\left(\frac{\mathcal{N}\tilde{V}^2\pi}{\sqrt{2\pi\sigma}} e^{-\frac{\mathcal{N}\tilde{V}^2}{2\sigma^2}} \right)$ with it, therefore as the value of Ω increases, the effects of disorder

vanishes exponentially and the contribution of the disorder to the linewidth goes down. In figures 11 and 12 we plot the absorption cross-section with varied values of σ keeping Ω constant. We can observe from Fig. 11 that as σ increases the peak position shifts and the lineshape is modified. But as shown in Fig. 12 for a higher value of Ω there is hardly any effect of σ on the lineshape. Therefore when $\epsilon_a = \epsilon_c$, under the condition $\Omega \gg \frac{\gamma_a + \gamma_c}{2} \gg \sigma$ the effect of disorder is negligible. This result echoes the findings of Houdré [32].

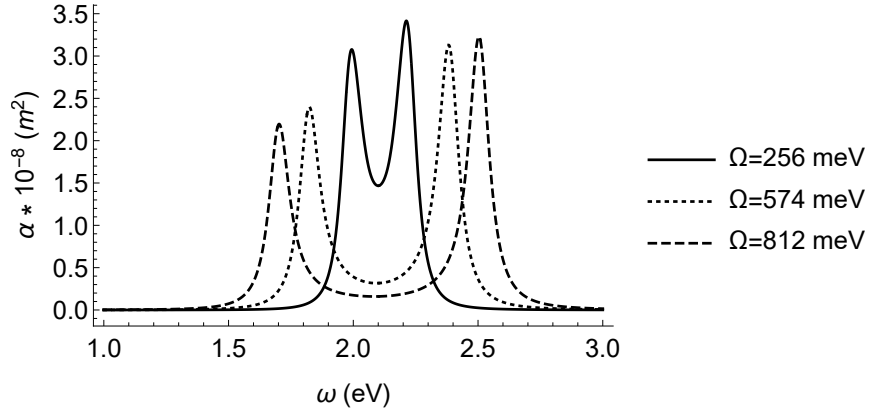


Figure 10: Plot for absorption cross-section $\alpha v/s \omega$ for varied value of Ω . Following values were used: $\epsilon_c = 2.1 eV$, $\epsilon_a = \epsilon_c$, $\tilde{V} = 4.06 \times 10^{-14} eVm^{3/2}$, $\sigma = 0.01\epsilon_a$, $\gamma_a = 0.3 meV$ and $\gamma_c = 0.1 eV$.

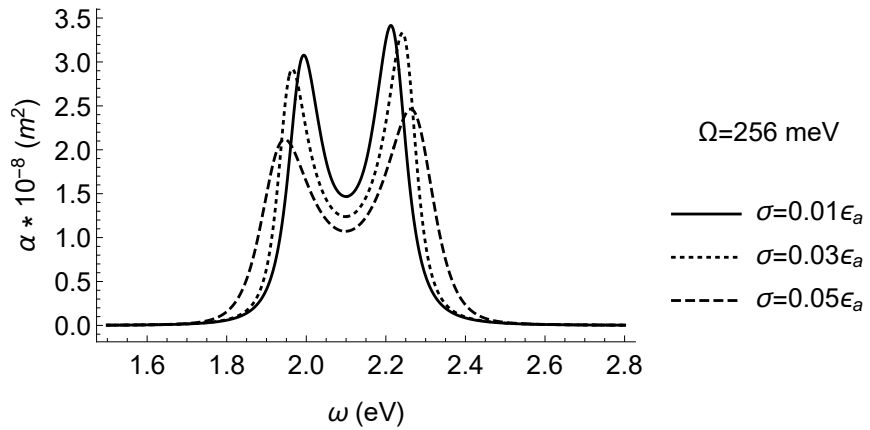


Figure 11: Plot for absorption cross-section $\alpha v/s \omega$ for varied value of σ . Following values were used: $\epsilon_c = 2.1 eV$, $\epsilon_a = \epsilon_c$, $\tilde{V} = 4.06 \times 10^{-14} eVm^{3/2}$, $\Omega = 256 meV$, $\gamma_a = 0.3 meV$ and $\gamma_c = 0.1 eV$.

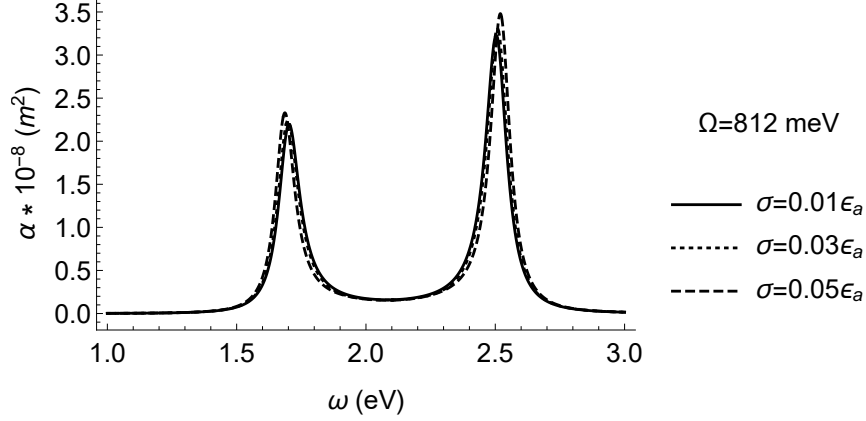


Figure 12: Plot for absorption cross-section α v/s ω for varied value of σ . Following values were used: $\epsilon_c = 2.1 eV$, $\epsilon_a = \epsilon_c$, $\tilde{V} = 4.06 \times 10^{-14} eVm^{3/2}$, $\Omega = 812 meV$, $\gamma_a = 0.3 meV$ and $\gamma_c = 0.1 eV$.

V. MODEL II: $V_i = V(\theta_i, z_i)$

The next situation we consider has orientational and position dependent coupling i.e., $V_i = V \cos(\theta_i) \sin(kz_i/L)$. θ_i is the angle between the electric field and transition dipole moment of the i^{th} molecule. The $\sin(kz_i/L)$ term accounts for the spatial variation of the electric field in the cavity of length L . ξ_i is assumed to be identically distributed Gaussian random variables with the probability distribution same as the one considered in Model I. As a result, we get

$$\langle \Sigma(\omega) \rangle = \frac{V^2}{4\pi L} \int_0^\pi \int_0^L \int_0^{2\pi} d\theta_i d\phi_i dz_i \sum_i \frac{\sin(\theta_i) \cos(\theta_i)^2 \sin(kz_i)^2}{\omega - \epsilon_i}. \quad (49)$$

Averaging over the angles and length will give us:

$$\langle \Sigma(\omega) \rangle = \frac{V^2}{6} \sum_i \frac{1}{\omega - \epsilon_i}. \quad (50)$$

This means that effectively the only result of orientational and positional averaging is to reduce the coupling per molecule by a factor of $\sqrt{6}$.

A. The Absorption Spectrum for Model II

Using the general interaction Hamiltonian given by Eq. (43), the absorption cross-section can be written as:

$$\alpha = \frac{\omega}{2\epsilon_0 c \hbar} \int_{-\infty}^{\infty} e^{i\omega t} \langle g | \hat{H}_{int}(t) \hat{H}_{int} | g \rangle dt \quad (51)$$

For this case the definition of $|mol\rangle$ needs to be modified. Now it is given by

$$|mol\rangle = F \sum_i \hat{\boldsymbol{\mu}}_i \cdot \mathbf{E}_i |g\rangle, \quad (52)$$

where $\hat{\boldsymbol{\mu}}_i = \boldsymbol{\mu}_i |g\rangle \langle e_i| + \boldsymbol{\mu}_i^* |e_i\rangle \langle g|$ and F is the normalization constant given by:

$$F^2 \sum_i |\boldsymbol{\mu}_i \cdot \mathbf{E}_i|^2 = 1 \quad (53)$$

Using this definition for $|mol\rangle$ we can rewrite Eq. (51) as

$$\alpha = \frac{\omega}{2\epsilon_0 c \hbar F^2} \int_{-\infty}^{\infty} e^{i\omega t} \langle mol | e^{-iHt/\hbar} | mol \rangle e^{iE_g t/\hbar} dt \quad (54)$$

$$= -\frac{\omega}{\epsilon_0 c \hbar F^2} \text{Im} \{G_{mol,mol}(\omega)\}. \quad (55)$$

Since F contains the information over orientation and spatial distribution we substitute it back and average over length and angle,

$$\alpha = -\frac{\omega}{\epsilon_0 c \hbar} \sum_i |\boldsymbol{\mu}_i \cdot \mathbf{E}_i|^2 \text{Im} \{G_{mol,mol}(\omega)\} \quad (56)$$

To determine $G_{mol,mol}(\omega)$ we re-write Eq. (30)

$$\underline{\underline{G}}_M(\omega^+) = \left[\omega^+ - \underline{\underline{\epsilon}}_M - \frac{\underline{\underline{V}}^\dagger \underline{\underline{V}}}{\omega^+ - \epsilon_c} \right]^{-1}. \quad (57)$$

Using Eq. (52) we can write the operator corresponding to $\underline{\underline{V}}^\dagger \underline{\underline{V}}$ in the form $F^{-2} |mol\rangle \langle mol|$, this gives us,

$$\hat{G}_M(\omega^+) = \left[\omega^+ - \hat{\epsilon}_M - \frac{F^{-2} |mol\rangle \langle mol|}{\omega^+ - \epsilon_c} \right]^{-1}. \quad (58)$$

Similar to the procedure for model I we can follow the steps to get:

$$\begin{aligned} G_{mol,mol}(\omega^+) &= \left\{ 1 - \frac{F^{-2} \langle mol | ([\omega^+ - \hat{\epsilon}_M]^{-1}) | mol \rangle}{\omega^+ - \epsilon_c} \right\}^{-1} \langle mol | [\omega^+ - \hat{\epsilon}_M]^{-1} | mol \rangle \\ &= \left\{ 1 - \frac{1}{\omega^+ - \epsilon_c} \sum_i \frac{|\boldsymbol{\mu}_i \cdot \mathbf{E}_i|^2}{\omega^+ - \epsilon_i} \right\}^{-1} F^2 \sum_i \frac{|\boldsymbol{\mu}_i \cdot \mathbf{E}_i|^2}{\omega^+ - \epsilon_i} \end{aligned}$$

The average over orientation and length are performed with an approximation that since the terms are all squares of $|\boldsymbol{\mu}_{eg,i} \cdot \mathbf{E}_i|$, we can individually average over each term. On averaging,

$$G_{mol,mol}(\omega^+) = \left\{ 1 - \frac{1}{\omega^+ - \epsilon_c} \langle \Sigma(\omega) \rangle \right\}^{-1} \frac{6}{NV^2} \langle \Sigma(\omega) \rangle$$

Here, $\langle \Sigma(\omega) \rangle$ is used as given in Eq. (50). With this result the absorption cross-section averaged over the length and orientation is,

$$\alpha = -\frac{\omega}{6\epsilon_0 c \hbar} N |\boldsymbol{\mu}|^2 \text{Im} \{ G_{mol,mol}(\omega) \}. \quad (59)$$

VI. CONCLUSIONS

A general solution for Tavis-Cummings model for a system with energetic disorder which follows a Gaussian distribution is provided in this work. Analytical solutions are obtained in the limit of large \mathcal{N} for a simple system where coupling is same for all the molecules and for a general system where coupling depends in the position and orientation of the molecules. Conditions for the existence of the polaritonic states is derived. A general expression for the polaritonic energies correct upto second order in disorder is derived. For the case where $\epsilon_a = \epsilon_c$, it is found that increase in disorder leads to an increase in the Rabi splitting. In general, polaritonic states are found to be very stable against disorder. They would always exist if the number density of molecules is sufficiently large. Our calculation of the absorption spectrum shows that disorder causes the dark states to turn grey. However, in the case where Rabi splitting is sufficiently large, disorder plays almost no role in the line width and in this limit the line width is dominated by lifetime effects. Orientational and position dependence of the coupling is shown to effectively renormalize the coupling strength.

VII. ACKNOWLEDGEMENTS

The authors thank Prof. Srihari Keshavamurthy (IITK) for his wonderful lectures titled ‘‘Chemistry with Quantum Light’’. This work is a result of an after lecture discussion with

him and Prof. Madhav Ranganathan (IITK) and the authors are grateful to both of them.

- [1] Anoop Thomas, Jino George, Atef Shalabney, Marian Dryzhakov, Sreejith J. Varma, Joseph Moran, Thibault Chervy, Xiaolan Zhong, Eloise Devaux, Cyriaque Genet, James A. Hutchison, and Thomas W. Ebbesen. Ground-state chemical reactivity under vibrational coupling to the vacuum electromagnetic field. *Angewandte Chemie International Edition*, 55(38):11462–11466, August 2016. I
- [2] A. Thomas, L. Lethuillier-Karl, K. Nagarajan, R. M. A. Vergauwe, J. George, T. Chervy, A. Shalabney, E. Devaux, C. Genet, J. Moran, and T. W. Ebbesen. Tilting a ground-state reactivity landscape by vibrational strong coupling. *Science*, 363(6427):615–619, February 2019. I
- [3] Kenji Hirai, Rie Takeda, James A. Hutchison, and Hiroshi Uji-i. Modulation of Prins Cyclization by Vibrational Strong Coupling. *Angewandte Chemie - International Edition*, 59(13):5332–5335, 2020. I
- [4] Vanessa N. Peters, Md Omar Faruk, Joshua Asane, Rohan Alexander, D’angelo A. Peters, Srujana Prayakarao, Sangeeta Rout, and M. A. Noginov. Effect of strong coupling on photodegradation of the semiconducting polymer p3ht. *Optica*, 6(3):318, March 2019.
- [5] Battulga Munkhbat, Martin Wersall, Denis G. Baranov, Tomasz J. Antosiewicz, and Timur Shegai. Suppression of photo-oxidation of organic chromophores by strong coupling to plasmonic nanoantennas. *Science Advances*, 4(7):9552, July 2018. I
- [6] Robrecht M. A. Vergauwe, Anoop Thomas, Kalaivanan Nagarajan, Atef Shalabney, Jino George, Thibault Chervy, Marcus Seidel, Eloise Devaux, Vladimir Torbeev, and Thomas W. Ebbesen. Modification of enzyme activity by vibrational strong coupling of water. *Angewandte Chemie*, 131:15468–15472, 10 2019. I
- [7] Xiaolan Zhong, Thibault Chervy, Shaojun Wang, Jino George, Anoop Thomas, James A. Hutchison, Eloise Devaux, Cyriaque Genet, and Thomas W. Ebbesen. Non-radiative energy transfer mediated by hybrid light-matter states. *Angewandte Chemie - International Edition*, 55(21):6202–6206, 2016. I
- [8] Xiaolan Zhong, Thibault Chervy, Lei Zhang, Anoop Thomas, Jino George, Cyriaque Genet, James A. Hutchison, and Thomas W. Ebbesen. Energy Transfer between Spatially Separated

- Entangled Molecules. *Angewandte Chemie - International Edition*, 56(31):9034–9038, 2017. I
- [9] David M. Coles, Niccolo Somaschi, Paolo Michetti, Caspar Clark, Pavlos G. Lagoudakis, Pavlos G. Savvidis, and David G. Lidzey. Polariton-mediated energy transfer between organic dyes in a strongly coupled optical microcavity. *Nature Materials*, 13(7):712–719, May 2014. I
- [10] Katherine Akulov, Dan Bochman, Adina Golombek, and Tal Schwartz. Long-distance resonant energy transfer mediated by hybrid plasmonic–photonic modes. *The Journal of Physical Chemistry C*, 122(28):15853–15860, June 2018. I
- [11] Thomas W. Ebbesen. Hybrid light–matter states in a molecular and material science perspective. *Accounts of Chemical Research*, 49(11):2403–2412, October 2016. I
- [12] James A. Hutchison, Tal Schwartz, Cyriaque Genet, Eloise Devaux, and Thomas W. Ebbesen. Modifying chemical landscapes by coupling to vacuum fields. *Angewandte Chemie International Edition*, 51(7):1592–1596, January 2012.
- [13] E. Orgiu, J. George, J. A. Hutchison, E. Devaux, J. F. Dayen, B. Doudin, F. Stellacci, C. Genet, J. Schachenmayer, C. Genes, G. Pupillo, P. Samorì, and T. W. Ebbesen. Conductivity in organic semiconductors hybridized with the vacuum field. *Nature Materials*, 14(11):1123–1129, September 2015. I
- [14] J. J. Pietron, K. P. Fears, J. C. Owrutsky, and B. S. Simpkins. Electrochemical modulation of strong vibration–cavity coupling. *ACS Photonics*, 7(1):165–173, December 2019. I
- [15] Shaelyn R. Casey and Justin R. Sparks. Vibrational strong coupling of organometallic complexes. *Journal of Physical Chemistry C*, 120:28138–28143, 12 2016. I
- [16] Javier Galego, Clàudia Climent, Francisco J. Garcia-Vidal, and Johannes Feist. Cavity Casimir-Polder Forces and Their Effects in Ground-State Chemical Reactivity. *Physical Review X*, 9(2):1–22, 2019. I
- [17] Vladimir P. Zhdanov. Vacuum field in a cavity, light-mediated vibrational coupling, and chemical reactivity. *Chemical Physics*, 535(March):110767, 2020.
- [18] Jorge A. Campos-Gonzalez-Angulo and Joel Yuen-Zhou. Polaritonic normal modes in transition state theory. *The Journal of Chemical Physics*, 152:161101, 4 2020. I
- [19] Denis G. Baranov, Martin Wersall, Jorge Cuadra, Tomasz J. Antosiewicz, and Timur Shegai. Novel nanostructures and materials for strong light-matter interactions. *ACS Photonics*, 5:24–42, 1 2018. I

- [20] Johannes Flick, Nicholas Rivera, and Prineha Narang. Strong light-matter coupling in quantum chemistry and quantum photonics. *Nanophotonics*, 7(9):1479–1501, September 2018.
- [21] Felipe Herrera and Jeffrey Owrutsky. Molecular polaritons for controlling chemistry with quantum optics. *Journal of Chemical Physics*, 152, 3 2020.
- [22] Felipe Herrera and Frank C. Spano. Theory of Nanoscale Organic Cavities: The Essential Role of Vibration-Photon Dressed States. *ACS Photonics*, 5(1):65–79, 2018.
- [23] Manuel Hertzog, Mao Wang, Jurgen Mony, and Karl Borjesson. Strong light-matter interactions: A new direction within chemistry. *Chemical Society Reviews*, 48:937–961, 2 2019.
- [24] Derek S. Wang and Susanne F. Yelin. A roadmap toward the theory of vibrational polariton chemistry. *ACS Photonics*, 8:2818–2826, 10 2021.
- [25] Raphael F. Ribeiro, Luis A. Martinez-Martinez, Matthew Du, Jorge Campos-Gonzalez-Angulo, and Joel Yuen-Zhou. Polariton chemistry: controlling molecular dynamics with optical cavities. *Chemical Science*, 9:6325–6339, 2018.
- [26] Johannes Feist, Javier Galego, and Francisco J. Garcia-Vidal. Polaritonic chemistry with organic molecules. *ACS Photonics*, 5:205–216, 1 2018. I
- [27] Felipe Herrera and Frank C. Spano. Cavity-Controlled Chemistry in Molecular Ensembles. *Physical Review Letters*, 116(23):1–6, 2016. I
- [28] Gregory D. Scholes. Polaritons and excitons: Hamiltonian design for enhanced coherence: Hamiltonian design for coherence. *Proceedings of the Royal Society A: Mathematical, Physical and Engineering Sciences*, 476, 10 2020. I
- [29] T. Botzung, D. Hagenmuller, S. Schutz, J. Dubail, G. Pupillo, and J. Schachenmayer. Dark state semilocalization of quantum emitters in a cavity. *Physical Review B*, 102, 10 2020. I
- [30] Matthew Du and Joel Yuen-Zhou. Can dark states explain vibropolaritonic chemistry? *Arxiv*, 4 2021. I
- [31] Nahum C. Chavez, Francesco Mattiotti, J. A. Mendez-Bermudez, Fausto Borgonovi, and G. Luca Celardo. Disorder-enhanced and disorder-independent transport with long-range hopping: Application to molecular chains in optical cavities. *Physical Review Letters*, 126, 4 2021. I
- [32] R. Houdré, R. P. Stanley, and M. Ilegems. Vacuum-field rabi splitting in the presence of inhomogeneous broadening: Resolution of a homogeneous linewidth in an inhomogeneously broadened system vacuum-field rabi splitting in the presence of inhomogeneous broadening:

- Resolution of a homogeneous linewidth in an inhomogeneously broadened system. *Physical Review A*, 53:2711–2715, 1996. I, IV A, IV A 4
- [33] Michael Tavis and Frederick W. Cummings. Exact solution for anN-molecule—radiation-field hamiltonian. *Physical Review*, 170(2):379–384, June 1968. I, II
- [34] Michael Tavis and Frederick W. Cummings. Approximate solutions for anN-molecule-radiation-field hamiltonian. *Physical Review*, 188(2):692–695, December 1969. I, II
- [35] P. W. Anderson. Localized magnetic states in metals. *Physical Review*, 124(1):41–53, October 1961. II
- [36] R.D. Mattuck. *A Guide to Feynman Diagrams in the Many-Body Problem: Second Edition*. Dover Books on Physics. Dover Publications, 2012. II
- [37] <https://mathworld.wolfram.com/dawsonintegral.html>. III
- [38] G.C. Schatz and M.A. Ratner. *Quantum Mechanics in Chemistry*. Dover Books on Chemistry. Dover Publications, 2012. IIIB
- [39] C.A. Coulson and R. McWeeny. *Coulson’s Valence*. Oxford Chemistry Series. Oxford University Press, 1979. IV A